

# A high-spatial-resolution fiber-optic-coupled CMOS imager with novel scintillator for high-energy x-ray applications

Robin M. Baur<sup>1,2</sup>, Mark W. Tate<sup>3</sup>, Darren S. Dale<sup>2</sup>, Sol M. Gruner<sup>1,2,3,4</sup>

<sup>1</sup> Department of Physics, Cornell University, Ithaca NY 14853 USA

<sup>2</sup> Cornell High Energy Synchrotron Source, Cornell University, Ithaca NY 14853 USA

<sup>3</sup> Laboratory of Atomic and Solid-State Physics, Cornell University, Ithaca NY 14853 USA

<sup>4</sup> Kavli Institute at Cornell for Nanoscale Science, Cornell University, Ithaca NY 14853 USA

E-mail: [rbaur@physics.cornell.edu](mailto:rbaur@physics.cornell.edu)

**Abstract.** A fast, high-spatial-resolution detector for high-energy microscopy work is presented. The detector uses a 2160 x 2560 CMOS chip for fast framing (up to 100 Hz in full-frame mode), coupled by a fiber optic taper to a scintillating Terbium-doped fiber optic plate for excellent stopping power even at high energies. The field of view is 7mm × 8.6mm with a resolution of 9 microns. The sensitivity is 1 e-/x-ray at 35 keV, with a read noise of 2.5 e-/pixel. Standard characterization metrics including dark current, sensitivity, modulation transfer function, and detective quantum efficiency are presented, along with preliminary experimental results.

## 1. Introduction

In many x-ray detector systems, achieving a high spatial resolution comes at the cost of significant losses in detection efficiency. Settled-phosphor screens typically yield resolution comparable to their thickness [1], and while single-crystal films are instead limited by the acceptance cone of the coupling optics, they still have unacceptably low stopping power at high energies. With this detector, we decouple the scintillator thickness from the resolution by using a Terbium-doped fiber optic as the scintillator; in this case the resolution is set by the fiber optic pitch, while the stopping power may be quite high if the fiber optic block is sufficiently thick.

## 2. Design

This detector uses a CMOS imager rather than a CCD. The advantages of CMOS technology over CCDs are readout speed and electronic shuttering, allowing for very fast integration. The chip is a prototype TCAM model scientific CMOS imager from Fairchild Imaging, Inc., which has been discussed previously [2]. The on-chip pixel pitch is 6.5 microns. The chip has two halves of 1080 × 2560 pixels each, for a total of 2160 × 2560 pixels.

The chip is bonded with epoxy (Emerson & Cumming TRABOND F114) to a fiber optic taper (Incom Inc. formulation BLE-359-6) providing 1:2 magnification (3 micron to 6 micron

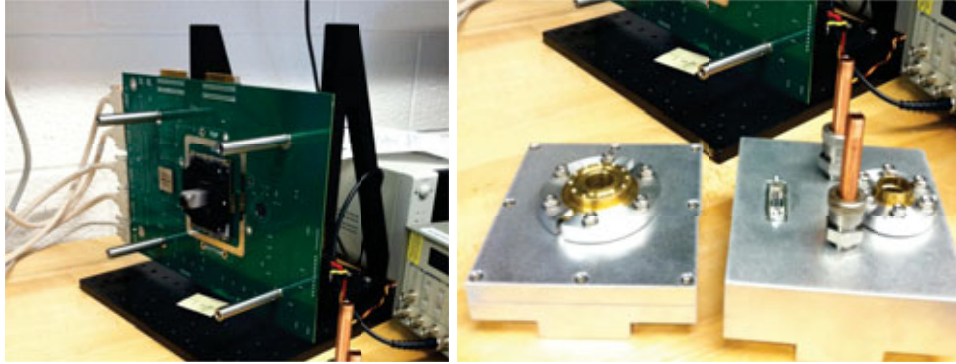


**Figure 1.** Left: The detector with the cryostat clamshell removed. Right: The cryostat housing.

fiber pitch) from the scintillator plane to the plane of the chip. The resulting field of view is  $7\text{mm} \times 8.6\text{mm}$  ( $V \times H$ ). This fiber optic taper is coupled by optical grease (Dow Corning Q2-3067) to a scintillating fiber optic plate, described in section 3.

The chip and fiber optics are housed in a custom cryostat which is held under vacuum ( $\sim 50$  mTorr) and which also contains a water-cooled cold finger whose temperature is controlled by a Peltier thermoelectric cooler (Melcor Inc. CP 1.4-127-045L). The detector assembly is shown in Fig. 1 with the housing removed.

### 3. Scintillator

The scintillator was custom-fabricated by Collimated Holes, Inc. for use with this detector. The core material is a Terbium-laced glass, doped with heavy elements for high stopping power ( $Z_{\text{eff}} = 31$ ; the precise formulation is proprietary) [3]. Each fiber is individually clad in a black glass to minimize optical crosstalk between neighboring fibers, which in turn minimizes point spread in the scintillator.

The scintillator fiber pitch is 6.2 microns center-to-center, with 5 micron x-ray sensitive cores. The block itself is 1cm thick, so the stopping power is close to 100% up to roughly 100 keV.

While uncoupled from the detector system, the scintillator was evaluated for light output, turn-on lag, and afterglow. Under 8 keV illumination, the light output was equivalent to that of an 11.7 micron single-crystal film of Europium-doped gadolinium gallium garnet (GGG:Eu). In lag and afterglow measurements, the turn-on and turn-off behavior of the scintillator was dominated by the mechanical transit of a shutter blade across the x-ray source, so the lag and afterglow decays must be at least as fast as the shutter blade, no slower than 2 ms.

### 4. Characterization

#### 4.1. Dark current, read noise, and dynamic range

The detector is operated at  $-20^\circ\text{C}$  to minimize dark current, but even at low temperature, the dark current is considerable,  $\sim 40 e^-/\text{s}$ . The read noise of the detector, measured by projecting the dark current data back to zero integration time, is  $2.5 e^-$ , after accounting for a  $50 e^-$  constant pedestal. The well depth of the chip is nominally  $30 ke^-$  per pixel, giving a dynamic range of 12000:1.

#### 4.2. Sensitivity

The sensitivity was measured at a synchrotron beamline (the A2 station at CHESS). The beam was slitted down to a  $2\text{mm} \times 2\text{mm}$  spot and passed through a calibrated ion chamber to determine the incident flux. The counts in the imaged beamspot were integrated, converted from

digital counts to electron signal, and divided by the measured flux to determine the sensitivity, after corrections for air absorption. The data for energies between 25 and 60 keV are shown in Fig. 2.

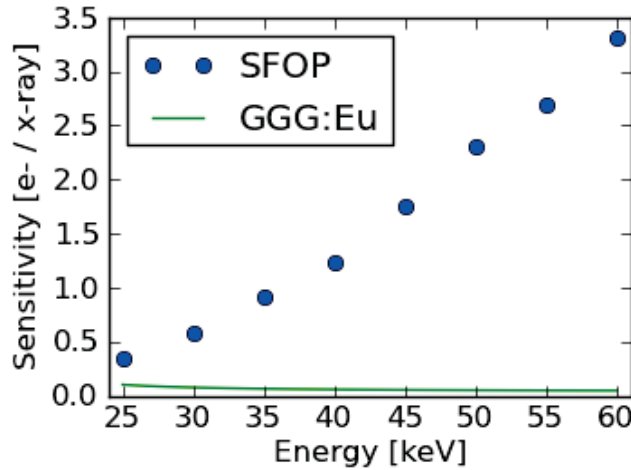


**Figure 2.** Sensitivity between 25 and 60 keV, with *predicted* performance of a similar system using an 11.7 micron GGG:Eu film for comparison. (SFOP: Scintillating Fiber Optic Plate)

4.3. Resolution

The resolution was measured according to ISO 12233 [4], with a knife edge tilted slightly with respect to the vertical pixel axis. This allows us to build up a super-resolved line spread function, whose Fourier transform gives the modulation transfer function (MTF) of the detector.

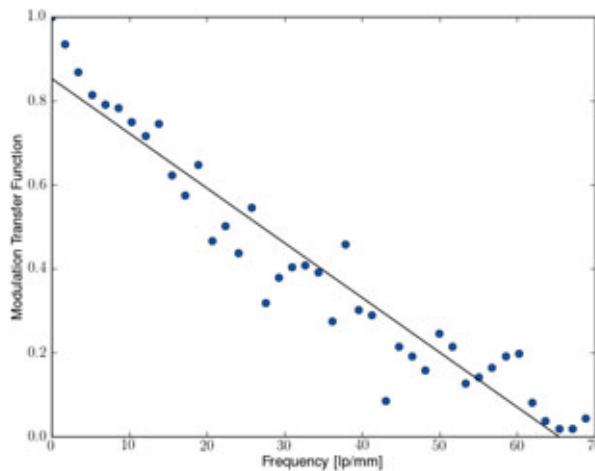


**Figure 3.** Modulation transfer function with straight-line fit as a guide to the eye.

Two possible metrics for resolution are the MTF at 50% and 10% of its peak value. For this measurement, the MTF50 was 27 lp/mm (37 microns) and the MTF10 was 57 lp/mm (17

microns). Both of these are less optimistic than the result of a Gaussian fit to the line spread function (not shown), which gives a FWHM resolution of 8.2 microns.

#### 4.4. Detective Quantum Efficiency

Detective quantum efficiency (DQE) is a measure of how much noise is present in the detected data relative to the amount of noise in the incident signal, given by the square of the ratio of the output and input signal-to-noise ratios:

$$\text{DQE} = \frac{(S/N)_{out}^2}{(S/N)_{in}^2}.$$

The DQE was measured as described in [5] by illuminating the detector at the A2 beamline and producing an array of uncorrelated spots. At various doses, two sequential exposures were taken and their sum and difference were calculated for each spot. The mean of the spot sums gives the output signal, while the standard deviation of the spot differences gives the output noise. The input x-ray signal, measured by integrating the counts in a calibrated ion chamber over the course of an exposure, is assumed to be Poisson, so that  $(S/N)_{in} = \sqrt{N_{ph}}$ . The resulting DQE data at several energies are shown in Fig. 4. The reason for the low DQE at 8 keV is not known, but is speculated to be due to a dead layer at the surface of the scintillator. These curves show that more work is needed to fully characterize and understand the fiber optic scintillator.

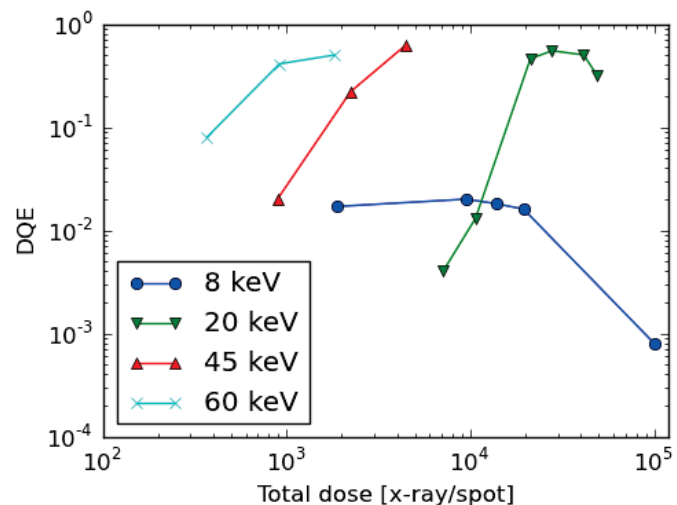


**Figure 4.** DQE at a range of energies. The truncation of the traditional parabolic shape is due to detector saturation.

#### Acknowledgments

The sCMOS chips and camera electronics were a gift of Brian Rodricks and Fairchild Imaging, Inc. The fiber optic tapers were a gift of Michael Detarando and Incom, Inc. The authors would also like to thank Duane Petrovitch and David Reaves of Fairchild Imaging for assistance with the camera control software. Detector development was supported by U.S. DOE grants FG02-97ER62443 & DE-FG02-10ER46693, and the Keck Foundation. CHESS is supported by the U.S. NSF and NIH-NIGMS under NSF award DMR-093638.

#### References

- [1] Gruner S, Tate M, and Eikenberry E 2002 *Rev. Sci. Instr.* **73** 2815-2842
- [2] Rodricks B *et al* 2009 *Proc. SPIE* **7449**, **7449Y** 1-11
- [3] Bueno C <http://www.collimatedholes.com/scindata.html>
- [4] ISO 12233, [http://www.iso.org/iso/catalogue\\_detail.htm?csnumber=33715](http://www.iso.org/iso/catalogue_detail.htm?csnumber=33715)
- [5] Tate M, Chamberlain D, and Gruner S 2005 *Rev. Sci. Instr.* **76** 081301